Plasma distribution of tetraphenylporphyrin derivatives relevant for Photodynamic Therapy: Importance and limits of hydrophobicity.

Benoît Chauvin, Athena Kasselouri, Bogdan I Iorga, Pierre Chaminade, Jean-Louis Paul, Philippe Maillard, Patrice Prognon

Title

Plasma distribution of tetraphenylporphyrin derivatives relevant for Photodynamic Therapy: importance and limits of hydrophobicity

Author names and affiliations

Benoît CHAUVIN [a,b], Athena KASSELOURI [a], Bogdan IORGA [c], Pierre CHAMINADE [a], Jean-Louis PAUL [d,e], Philippe MAILLARD [b], Patrice PROGNON [a]

[a] Univ. Paris-Sud, EA 4041, IFR 141, Faculté de Pharmacie, F-92296 Châtenay-Malabry, France

[b] Institut Curie, UMR 176 CNRS, Centre Universitaire, Univ Paris-Sud, F-91405 Orsay, France

[c] Institut de Chimie des Substances Naturelles, Gif sur Yvette, France

[d] AP-HP, Hôpital Européen Georges Pompidou, Service de Biochimie, Paris, France.

[e] Univ Paris-Sud, Laboratoire de Biochimie appliquée, EA 4529, 5 rue J-B. Clément, 92296 Châtenay-Malabry, France.

Benoît CHAUVIN : benoit.chauvin@u-psud.fr

Athena KASSELOURI : athena.kasselouri@u-psud.fr

Bogdan IORGA : bogdan.iorga@icsn.cnrs-gif.fr

Pierre CHAMINADE : pierre.chaminade@u-psud.fr

Jean-Louis PAUL : jean-louis.paul@u-psud.fr

Philippe MAILLARD : philippe.maillard@curie.fr

Patrice PROGNON : patrice.prognon@u-psud.fr

Corresponding author

Benoît CHAUVIN : benoit.chauvin@u-psud.fr

Laboratoire de Chimie Analytique, EA4041, IFR 141, Univ Paris-Sud, 5 rue J-B. Clément, 92296 Châtenay-Malabry, France

Tel: +33 1 46 83 58 49 Fax: +33 1 46 83 53 89

Present/permanent address

NA

Abstract

In the course of a Photodynamic Therapy (PDT) protocol, desagregation of the sensitizer upon binding to plasma proteins and lipoproteins is one of the first step following intraveinous administration. This step governs its subsequent biodistribution, and has even been evoked as possibly orientating mechanism of tumor destruction. It is currently admitted as being mainly dependent on sensitizer's hydrophobicity. In this context, as far as glycoconjugation, a promising strategy to improve targeting of retinoblastoma cells, confers to the sensitizer an amphiphilic character, we have studied the effect of this strategy on binding to plasma proteins and lipoproteins. With the exception of the majoritary protein-binding (more than 80%) of more hydrophilic *para*-tetraglycoconjugated derivatives, high-density lipoproteins (HDL) appear as main plasma carriers of the other amphiphilic glycoconjugated photosensitizers. This HDL-binding is a combined result of binding affinities (log Ka ranging from 4.90 to 8.77 depending on the carrier and the TPP derivative considered) and relative plasma concentrations of the different carriers. Evaluation of binding affinities shows that if hydrophobicity can account for LDL- and HDL-affinities, it is not the case for albumin-affinity. Molecular docking simulations show that, if interactions are mainly of hydrophobic nature, polar interactions such as hydrogen bonds are also involved. Those combination of interaction modalities should account for the absence of correlation between albumin-affinity and hydrophobicity. Taken together, our findings clarify the importance, but also the limits, of hydrophobicity's role in structure – plasma distribution relationship.

Keywords

meso-tetraphenylporphyrin, photodynamic therapy, plasma, lipoprotein, albumin, hydrophobicity

Abbreviations

TPP : 5,10,15,20-tetraphenylporphyrin*, meso*-tetraphenylporphyrin

MCR-ALS : Multivariate Curve Resolution – Alternating Least Squares

PDT : PhotoDynamic Therapy

DEG : Di Ethylene Glycol

TPP(*m*OH)$_3$: 5,10,15-tri-(*meta*-hydroxyphenyl)-20-phenylporphyrin

TPP(*m*OH)$_4$: 5,10,15,20-tetra-(*meta*-hydroxyphenyl)porphyrin

TPP(*m*O□GluOH)$_3$: 5,10,15-tri-(*meta*-O-□-D-glucopyranosyloxyphenyl)-20-phenylporphyrin

TPP(*m*O□GluOH)$_4$: 5,10,15,20-tetra-(*meta*-O-□-D-glucopyranosyloxyphenyl)porphyrin

TPP(*p*OH)$_3$: 5,10,15-tri(*para*-hydroxyphenyl)-20-phenylporphyrin

TPP(*p*OH)$_4$: 5,10,15,20-tetra-(*para*-hydroxyphenyl)porphyrin

TPP(*p*O□GalOH)$_3$: 5,10,15-tri(*para*-O-□-D-galactosyloxyphenyl)-20-phenylporphyrin

TPP(*p*O□GalOH)$_4$: 5,10,15,20-tetra-(*para*-O-□-D-galactosyloxyphenyl)porphyrin

TPP(*p*O□GluOH)$_4$: 5,10,15,20-tetra-(*para*-O-□-D-glucopyranosyloxyphenyl)porphyrin

TPP(*p*ODEGO□ManOH)$_3$: 5,10,15-tri{*para*-O-[(2-(2-O-□-D-mannosyloxy)-ethoxy)-ethoxy]-phenyl}-20-phenylporphyrin

1. Introduction

Photodynamic Therapy (PDT) is an emerging technique which combines administration of a drug, called photosensitizer, and exposure of targeted tissue to light of appropriate wavelength. Treatment effect results from the potency of the photosensitizer once activated by light to generate singlet oxygen and radical species responsible for cellular death. PDT has already proven its efficacy in the field of oncology for the treatment of lung, gastrointestinal or cutaneous tumours. It has also be applied to non-malignant diseases such as age-related macular degeneration [1]. In that case, transparency of ocular tissues to light makes PDT of particular interest. This property should also been exploited for the treatment of malignant ocular pathologies, such as retinoblastoma, the most frequent intraocular tumor in childhood. Indeed, besides poor efficiency for advanced tumors, currently available conservative treatments expose patients to a risk of developing secondary tumors [2]. PDT appears as promising, combining a physical selectivity (tissular volume illuminated) and a chemical one (tissular volume containing the photosensitizer). When applied to retinoblastoma tumors, photosensitizers developed for other pathologies have shown poor efficiencies and selectivities, leading to side-effects such as long lasting photosensitization of normal tissues. Design of new photosensitizers adapted to retinoblastoma appears necessary [3].

Our group is involved in the evaluation of glycoconjugation of tetrapyrrolic macrocycles. This strategy combines targeting of cellular sugar receptors and improvement of photosensitizer solubility. The former promotes selective destruction of malignant cells, the latter favors rapid elimination from healthy tissues. In vitro photocytotoxicity and in vivo pharmacokinetics studies have confirmed the potential interest of this approach [4, 5]. Efficacity of a glycoconjugated TPP, TPP(*p*ODEGO□ManOH)$_3$, has been attested in vivo, especially with a particular administration protocol (double drug dose with a 3 hour interval), which combines targeting of cancer cells and of blood vessels. Indeed, at the time of illumination, drug administered 10 min before is still present in the vicinity of blood vessels whereas drug

98 administered 3 hour before has reached tumor cells [6]. Destruction of blood vessels
99 indirectly kills tumor tissue, through deprivation of oxygen and nutriments [7].
100 Photo-induced destruction of blood vessels is of particular interest in the case of an
101 application of PDT to retinoblastoma as far as this tumor is considered as extremely sensitive
102 to vascular insufficiency [8]. However, this possible mechanism of action rises the question of
103 selectivity. This concept, defined as the ratio of sensitizer concentrations in tumor relative to
104 healthy adjacent tissue, must not be considered as the exclusive result of tumor cells
105 specificities. Tumor vasculature particularities could also be involved. Indeed, tumor
106 angiogenesis leads to the formation of permeable neo-vessels [9]. However, Roberts has
107 shown that this particular permeability is insufficient to account for selective retention of
108 photosensitizers. Excluding a possible difference in lymphatic drainage, he formulated the
109 hypothesis that selectivity results from a particular affinity of photosensitizers for endothelium
110 of neo-vessels, presuming an implication of drug carriers, such as albumin and lipoproteins
111 [10]. Binding to the latter has retained particular attention since the observation by Jori of a
112 strong correlation between fraction of photosensitizer bound to LDL and selectivity [11].
113 Overexpression of LDL-receptors by tumor cells and also by endothelial cells reinforces this
114 hypothesis [12]. If LDL-binding is associated to tumour cell delivery, binding of sensitizer to
115 high density lipoprotein (HDL) or albumin has been associated with vascular sequestration of
116 photosensitizer, leading to vascular damages upon photoactivation [13]. A strict correlation
117 between binding to a carrier and localization remains difficult to establish, localization being
118 time-dependent. Thus, biodistribution studies of BPD-MA conjugated to lipoproteins has
119 shown the role of plasma carriers in modulation of pharmacokinetics: conjugation to LDL
120 increases selectivity whereas conjugation to HDL delays tumor accumulation [14].
121 Plasma distribution studies have evidenced the major role of lipoproteins in photosensitizer
122 transport, compared with the albumin binding of most drugs [13, 15]. This particularity is
123 attributed to the high hydrophobic character of sensitizers. This property seems to govern
124 plasma distribution, as it is frequently considered that hydrophilic compounds bind to proteins
125 (especially albumin) and lipophilic ones to LDL. Amphiphilic derivatives present a tendency to

bind mainly to HDL [16]. In this point of view, glycoconjugation, which increases the solubility of the sensitizer and decreases its hydrophobicity, should affect interactions with plasma proteins and lipoproteins. Thus it appears essential to focus on the impact of the glycoconjugation on drug distribution between plasma components. This study covers ten meso-tetraphenylporphyrin derivatives, six of which are glycoconjugated according to different modalities, and thus different lipophilicities. The aim is, beyond a description of the relationship between structure and plasma distribution, to better understand factors governing interactions of TPP sensitizers with plasma proteins and lipoproteins.

2. Materials and Methods

2.1. Chemicals

TPP(*p*OH)$_4$ was purchased from Sigma-Aldrich® (Germany) and TPP(*m*OH)$_4$ from Frontier Scientific® (USA). All other porphyrins were synthesized according to previously published protocols [17-20]. Stock solutions were prepared in DMSO and kept in the dark at + 4°C. Theophylline, 5-phenyl-1H-tetrazole, indole, propiophenone and valerophenone were provided by Acros Organics (USA), benzimidazole, butyrophenone, colchicine, potassium bromide and ammonium acetate by Merck (Germany), acetophenone by Carlo Erba (Italia), 0.9 % sodium chloride solution by Aguettant (France). HPLC grade acetonitrile, methanol and dimethylsulfoxyde came from VWR (Germany), pH 7.4 PBS and human serum albumin from Sigma-Aldrich (Germany). Two different references of the latter (corresponding to different purification levels) were used, one is essentially fatty acid free (HSA), the other is not fatty acid free (HSAlip). Ultrapure water was provided by an Alpha-Q device (Millipore®, France). Human plasma was taken from normolipemic hemochromatosis patients.

2.2. Determination of Chromatographic Hydrophobicity Index (CHI)

The procedure proposed by Valko has been applied to the TPP derivatives [21]. CHI values of the two parent tri-hydroxylated compounds are not evaluable with this protocol. Calibration

153 set covered the log P range from -0.02 to 3.26: theophylline, 5-phenyl-1H-tetrazole,
154 benzimidazole, colchicine, 8-phenyltheophylline, indole, acetophenone, propiophenone,
155 butyrophenone, and valerophenone. HPLC measurements were performed on a Biotek
156 Kontron system, operated with Geminyx (version 1.91) software. Experiments were carried
157 out on a Modulo-cart QS uptisphere ODB column (Interchim, France), with the dimensions of
158 150 x 4.6 mm. The mobile phase, a gradient between of 50 mM ammonium acetate (pH
159 ranging from 7.0 to 7.3) and acetonitrile, was delivered at the flow rate of 1.0 $mL.min^{-1}$
160 according to the following program: 0-1.5 min, 0% acetonitrile; 1.5 -10.5 min, 0-100%
161 acetonitrile; 10.5- 11.5 min, 100% acetonitrile; 11.5-12.0 min, 0% acetonitrile; 12.0- 20.0 min,
162 0% acetonitrile. For every TPP studied, reference dataset was injected simultaneously with
163 the photosensitizer in a mixture of 50% acetonitrile and 50% aqueous ammonium acetate
164 buffer. Elution of the standards and of the photosensitizer were monitored respectively at 254
165 nm and 416 nm. Final CHI values for TPPs were the mean of three experiments, using CHI
166 values determined by Valko for reference dataset.
167

168 ## 2.3. Distribution in human plasma

169 After 24-hour incubation with one percent of a porphyrin solution in dimethylsulfoxide, plasma
170 samples were brought to the density of 1.21 $g.mL^{-1}$ with potassium bromide. Porphyrin final
171 molar concentration (3 µM) was in the order of magnitude of what should be expected *in vivo*
172 with an effective dose. Protein and lipoprotein fractions were separated by ultracentrifugation
173 (90 000 rpm, 8 h, 4°C) using a Beckman NVT 90 rotor in a Beckman XL 90 ultracentrifuge.
174 Separation of lipoproteins was performed with a density-gradient ultracentrifugation using a
175 five-step KBr/NaCl gradient (densities of 1.063, 1.042, 1.019 and 1.006 $g.mL^{-1}$ on top of
176 plasma and a 1.21 $g.mL^{-1}$ KBr solution) and centrifuging for 24 h (38 000 rpm, 4°C) using a
177 Beckman SW 41 rotor in a Beckman XL 90 ultracentrifuge. After ultracentrifugation, fractions
178 were collected using a system including a Density Gradient Fractionator ISCO Model 185, a
179 collector LKB Bromma – 2212 HELIRAC and a detector LKB Bromma – 2238 UVICORD S II
180 (continuous absorbance monitoring at 280 nm). An extraction was performed on the samples

according to the method proposed by Wang [22]. 1900 µL of a mixture dimethylsulfoxide – methanol 1:4 (v/v) was added to 100 µL of each fraction collected. After centrifugation (10 min, 4000 rpm), fluorescence intensity was read on the supernatant with a Perkin-Elmer LS-50B spectrofluorimeter, with an excitation wavelength set at 420 nm. Plasma distribution between the different fractions was calculated on the basis of those fluorescence intensities.

2.4. Spectroscopic study of interactions with plama proteins and lipoproteins

2.4.1. Preparation of LDL and HDL fractions

Human plasma density is adjusted to 1.019 $g.mL^{-1}$ with KBr. After 24 h centrifuging (45 000 rpm, 4°C), supernatant is removed and density of the remaining is further increased to 1.063 $g.mL^{-1}$ with KBr. After 48 h centrifuging (45 000 rpm, 4°C), two fractions are obtained, the upper one corresponding to LDL, the lower one to HDL. Molar concentrations of LDL and HDL particles were determined on the basis of apoprotein quantitation according to the method proposed by Ohnishi [23].

2.4.2. Sample preparation and conditions of spectra recording

An intermediate dilution of TPP stock solutions in pH 7.4 phosphate buffer saline (PBS) was used to prepare mixtures of a TPP with the studied plasma carrier (HSA, HSA-LIP, HDL ou LDL). Dimethylsulfoxide final proportion in this solution was 0.5 %. TPP final concentration was 1.10^{-7} M for fluorescence measurements and 5.10^{-7} M for absorption study. Transporter concentration varied from 0 to 1.10^{-4} M. The mixtures were kept in darkness at 37 ºC for 24 hours. UV – Visible absorption spectra were recorded on a Varian® Cary Bio 100 spectrophotometer (Australia), with an optical path of 10 mm and a slit width of 2 nm. Fluorescence emission spectra were recorded with a Perkin-Elmer LS-50B spectrofluorimeter, with an excitation wavelength set at 420 nm (excitation and emission slits equal to 7 nm).

2.4.3. Determination of binding constants

When compared with absorption spectroscopy, determination of binding constants by fluorimetry presents two advantages: the possibility of working with lower TPP concentrations (~10^{-7} M) than with absorption spectroscopy (~5.10^{-7} M), and the lower diffusion due to plasma carriers. Combined together, those two advantages widen the TPP – carrier ratio range possible to study. Classical binding of drugs to plasma proteins and lipoproteins is described by an equilibrium involving the free drug, the free carrier on the one side and the drug-carrier complex on the other side. Thus, if binding involves a change in drug fluorescence intensity at one wavelength, affinity constants can be determined through monitoring of fluorescence at this wavelength:

$$F = F_{free} + (F_{bound} - F_{free}) \times \frac{K_a \times [Carrier]}{1 + K_a \times [Carrier]} \quad \textbf{(1)}$$

where F_{free} and F_{bound} are fluorescence emission intensities respectively of the free and of the bound drug, [*Carrier*] the concentration of the drug carrier and K_a the affinity constant defined by the following relationship:

$$K_a = \frac{[Drug - Carrier]}{[Drug][Carrier]} \quad \textbf{(2)}$$

where [*Drug*] and [*Drug – Carrier*] are the respective concentrations of the free drug and of the drug-carrier complex. This method relies on the proportionnality of F_{free} and F_{bound} to the respective concentrations of these two forms, [*Drug*] and [*Drug – Carrier*]. However, in the particular case of TPP derivatives, this is not the case. Indeed, free drug is not an homogeneous form and covers in fact two different forms: an aggregated one (poorly fluorescent) and a solubilized one (moderately fluorescent).Then, fluorescence intensity of the free drug is no more directly proportional to its concentration, because it will depend on its agregation rate, which is probably inversely related with its concentration.

To overcome limitations of monowavelength monitoring in this particular case, multivariate curve resolution – alternating least squares (MCR-ALS) has been applied on fluorescence emission spectra recorded with different carrier concentrations [24]. MCR-ALS consists in the decomposition of this data matrix (D) into the product of two matrices: 1) a C matrix

containing concentration profiles of the different species, 2) a S matrix with their fluorescence spectra.

$$D = C \,.\, S^T + E \quad \textbf{(3)}$$

E matrix represents difference between experimental values and data predicted by the model, that is residuals. Data analysis method proposed by Diewok for MatLab [25] has been adapted here to R software [26]. Optimization is based on *als* algorithm contained in the ALS package [27]. High agregation of certain TPP derivatives combined with a strong affinity for some of the studied plasma carriers reduces contribution of the solubilized drug. In as far as fluorescence emission spectra of this particular species are the same whatever the carrier considered, a column-wise extended approach has been used to improve results. D matrix is constituted by spectra recorded on one TPP derivative with the four carriers studied : HSA, HSAlip, LDL, HDL. C and S matrices respectively contain concentration and spectra profiles of five species : the free solubilized drug and the four complexes formed by the TPP with each of the four carriers studied. Because of its poor fluorescence, the aggregated free drug is not included directly. Its presence is taken into account by applying no concentration closure constraint (sums of concentrations of the other species at each carrier concentration are not forced to be equal to one). For each carrier, concentration profile of the bound drug is adjusted to follow relationship (2), before subsequent spectra optimization. When further optimizations no more reduce residues' amount, the four binding constants are determined by non-linear regression of the concentration profile with equation (2).

2.5. Molecular docking simulations

Blind docking of TPP derivatives into human serum albumin (PDB code 1AO6) was performed with AutoDock Vina 1.0 (exhaustiveness value of 100 and maximum output of 20 structures) [28]. Unsubstituted TPP crystal structure has been downloaded from the Cambridge Structural Database (MOLFEZ). After substituents' addition with UCSF Chimera, ligands were prepared for docking using AutoDock Tools to calculate Gasteiger charges and set active torsions (the four bonds between porphyrin core and phenyls, all rotatable bonds

between the phenyl and the sugar residue). UCSF Chimera was used to visualize dockings, calculate contact surfaces and monitor hydrogen bonds. The selection of the main binding depended on the frequence of the different sites among the twenty output structures.

3. Results

3.1. Hydrophobicity of TPPs

As expected, glycoconjugation induces a decrease of hydrophobicity relative to the hydroxylated parent compound. Moreover, hydrophobicity is further reduced with increasing number of sugar residues. If these conclusions apply both to *para* and *meta* series, it is to note that *para*-derivatives are less hydrophobic than their *meta* isomers. Thus, CHI of TPP(*p*O□GluOH)$_4$ (28.3) is lower than that of the TPP(*m*O□GluOH)$_4$ (39.3). This also holds true for hydroxylated compounds, when comparing TPP(*p*OH)$_4$ (CHI=100.2) and TPP(*m*OH)$_4$ (117.2). Because of minor differences of hydrophobicity between mannose and galactose residues, the large CHI increase between TPP(*p*O□GalOH)$_3$ (CHI=40.8) and TPP(*p*ODEGO□ManOH)$_3$ (CHI=62.4) should be attributed to the presence of a spacer between the sugar and the phenyle. The *para*-derivative with the spacer is even more hydrophobic than the *meta*-triglycoconjugated derivative, TPP(*m*O□GluOH)$_3$ (CHI=55.7).

3.2. Distribution in human plasma

For eight of the ten studied compounds, more than 75 % of the sensitizer is found in lipoproteic fraction. Exceptions to this rule are constituted by the two *para*-tetraglycoconjugated derivatives, TPP(*p*O□GalOH)$_4$ and TPP(*p*O□GluOH)$_4$, lone compounds to be mainly bound – about 80% – to the proteic fraction. This behavior is particular striking when compared with the quite exclusive lipoproteic transport of the *meta*-tetraglycoconjugated derivative. Among compounds majoritary bound to lipoproteins, the *para*-triglycoconjugated TPP(*p*O□GalOH)$_3$ presents a significantly higher protein-bound fraction than other compounds, including TPP(*p*ODEGO□ManOH)$_3$. Drug binding to proteic

fraction concerns one quarter of the former but is negligeable in the case of the latter (less than 6%). This comparison shows that inclusion of a spacer between the sugar and the phenyle has a dramatic effect on plasma distribution.

HDL are main lipoproteic carriers of photosensitizers. Indeed, with the exception of TPP(*p*O□GalOH)$_4$ and TPP(*p*O□GluOH)$_4$, those structures bind more than half of sensitizer present in plasma. Binding to LDL is always minoritary, the highest proportion being reached with the TPP(*m*O□GluOH)$_4$.

3.3. Binding constants toward plasma proteins and lipoproteins

Binding of TPPs to plasma carriers induces spectral modifications, accounting for the disruption of TPPs aggregates upon formation of a complex between the TPP and the carrier. Those equilibria can be followed by absorption or fluorescence spectroscopies. In the absence of plasma carrier, absorption spectrum of TPP(*p*O□GalOH)$_3$ presents a large Soret band at 417 nm, with a distinct shoulder at 437 nm, the latter resulting from the formation of J-aggregates. HSA addition leads to the disappearance of the 437-nm shoulder characteristic of aggregates, and to the appearance of a new intense band at 422 nm, which attests for the formation of the complex. Concerning fluorescence spectroscopy, binding of TPP to HSA induces a slight modification of spectral shape but a significant increase in fluorescence intensity.

If all TPP are likely to bind to LDL, HDL and HSA, affinities dramatically vary according to carrier and substitution of the TPP core. However, it is remarkable to observe that, whatever the TPP considered, affinities towards the different plasma carriers decrease when passing from LDL to HDL and finally to HSA (whether fatty acid free or not). Even compounds mainly bound to proteins in plasma (TPP(*p*O□GalOH)$_4$ and TPP(*p*O□GluOH)$_4$) present a higher affinity for LDL than for other studied plasma components. Those *para*-derivatives present higher affinity constants towards HSA and HSAlip than their *meta*-homologous, an observation that applies whatever the substitution considered.

An other noteworthy result is the large difference in binding affinities for compounds with similar plasma distribution. That is the case of TPP(*p*OH)$_4$ and TPP(*p*ODEGO□ManOH)$_3$, two compounds bound at ~85 % to HDL. Binding affinity to LDL and HSA is ten-fold higher for the former than for the latter. When compared with TPP(*p*O□GalOH)$_3$, TPP(*p*ODEGO□ManOH)$_3$ presents the same order of magnitude in their binding constants towards LDL and HDL. Spacer mainly affects binding to HSA, decreasing ten fold binding affinities, which could account for the lower protein binding of this compound when compared with TPP(*p*O□GalOH)$_3$.

3.4. Molecular docking simulations

Depending on their substitution, TPPs interact at different locations on the HSA molecule. The most noticeable result is the impossibility for those bulky structures to insert into the two hydrophobic pockets that constitute Sudlow binding sites common to most drugs. It is difficult to privilegiate one binding site for non-glycoconjugated TPPs. Those structures are spread at different locations depending on their substitution. On the opposite, glycoconjugated porphyrins present preferential clusters.

If considering glycoconjugated porphyrins, the most noticeable result is the drastic effect of sugar position. Sugar nature and number don't seem to affect binding location. The two *meta* derivatives, TPP(*m*O□GluOH)$_3$ and TPP(*m*O□GluOH)$_4$, bind on the same location in the inter-domain crevice whereas the three *para* derivatives without spacer share the same binding site. For the latter three compounds, TPP(*p*O□GalOH)$_3$, TPP(*p*O□GalOH)$_4$ and TPP(*p*O□GluOH)$_4$, the tetrapyrrole is located between residues Q104 and K466, with two phenyles of both sides of residue K106.

TPP(*m*O□GluOH)$_3$ binds between subdomains Ib and IIIa, with the TPP core located below residue R114. The three sugar residues insert into three polar pockets: i) the first formed by residues R114, R117, R186 and K519, ii) the second constituted by residues N109, S419, T422, K466 and T467, iii) the third composed by amino acids D108, H146, K190, R197 and

342 Q459. In the case of the tetraglycoconjugated TPP(*m*O□GluOH)$_4$, three sugars insert in the
343 same pockets, the fourth interacting with K524.
344 Of particular interest is the modulation of distribution pattern induced by the presence of the
345 spacer. If this particularity doesn't prevent TPP(*p*ODEGO□ManOH)$_3$ from interacting at the
346 same location than TPP(*p*O□GalOH)$_3$), it favors binding on a site next to that of
347 TPP(*m*O□GluOH)$_3$, on a site inacessible to the tri-paraglycoconjugated derivative without
348 spacer (TPP(*p*O□GalOH)$_3$). In this particular conformation, the tetrapyrrole is close to
349 residue P421, one sugar is located between residues Q33 and E86, one other between
350 residues K419 and K500. The last mannose residue inserts into the third polar pocket
351 described for TPP(*m*O□GluOH)$_3$.
352 The fact that sugar residues are suceptible to insert into polar pockets in the case of
353 TPP(*p*ODEGO□ManOH)$_3$ or *meta*-derivatives results in an higher contribution of the
354 substituent in the interaction surface for those derivatives (table 3). For those particular
355 structures, TPP ring is less accessible to solvent than in the case of *para* derivatives without
356 spacer. This latter fact is confirmed by the percentage of the TPP nucleus involved in the
357 interaction (table 3). Interaction surfaces increase with increasing surfaces of the TPP
358 derivatives. The main exception to this rule is *para*-tetraglycoconjugated derivatives, their
359 interface surfaces being lower than that of TPP(*p*O□GalOH)$_3$. This fact probably results from
360 the rigidity of *para*-conformation, which induces a reduced possibility to insert into favorable
361 pockets upon increasing molecular volume. Indeed, flexibility of *meta*-derivatives confers to
362 those derivatives the ability to form higher interface surfaces with the protein than *para*
363 derivatives. Analysis of interaction modalities shows that TPPs interact with HSA mainly
364 through hydrophobic interactions but also through hydrogen bonds. The latter, which are
365 stronger interactions, mainly concern glycoconjugated compounds, due to their increased
366 number of hydroxyle groups.
367

368 ## 4. Discussion

369 ### 4.1. Plasma distribution of photosensitizers

Plasma distributions of glycoconjugated TPPs are consistent with common considerations on the relationships between plasma distribution and hydrophobicity. Differences in hydrophobicity mainly result from differences in exposure of the TPP ring due to the presence of polar substituents. This principle accounts for the effect of substituent's nature and number but also position. Indeed, para-substitution confers to the molecule a planar conformation different from the globular conformation resulting from meta-substitution. The latter allows an easier access to the hydrophobic TPP core.

Binding to the proteic fraction of *para*-tetraglycoconjugated derivatives can be explained by the more pronounced hydrophilic character of those compounds. TPP(*p*O□GalOH)$_3$ presents an intermediate CHI and an intermediate behavior between hydrophilic protein-bound derivatives and more hydrophobic compounds quite exclusively bound to lipoproteins. The latter compounds present the typical behavior of amphiphilic compounds, mainly bound to HDL. Binding to LDL concerns always a minoritary proportion of TPPs on the studied series. The effect of *para*-glycoconjugation appears similar to that of *para*-sulfonation as described by Kongshaug [13]: only the tetrasubstituted compound binds mainly to proteins, other derivatives (whether mono-, di- or tri-sulfonated) bind mainly to lipoproteins, majoritarily HDL. Binding to LDL is commonly associated with the hydrophobic character of TPPs. However, in our series, there is no correlation between proportion bound to LDL and CHI. This finding is similar to that described in the case of the sulfonated TPPs : a disulfonated TPP presents a higher proportion bound to LDL than the more hydrophobic monosulfonated derivative [13]. Moreover, in our series, similar hydrophobicities do not imply similar distribution patterns, as can be evinced by comparing TPP(*p*O□GalOH)$_3$ and TPP(*m*O□GluOH)$_4$.

4.2. From plasma distribution to binding constants

The most striking conclusion of the comparison between plasma distribution and binding constants is that even compounds predominantly bound to proteins in plasma have a higher affinity towards lipoproteins, especially LDL. This striking result recalls that relative affinities towards separated plasma carriers is just a part of its plasma distribution, the latter being

also the result of relative concentrations of plasma carriers. Involvement of plasma protein and lipoprotein concentrations has been underlined by Kongshaug in the case of hematoporphyrin [29]. This compound presents a majoritary binding to HDL in plasma, despite a higher affinity towards LDL than towards HDL. Thus, plasma distributions of TPP(*p*O□GalOH)$_4$ and TPP(*p*O□GluOH)$_4$ are not the consequence of a particular affinity towards albumin, but the result of a ratio of affinities towards lipoproteins and albumin not high enough to overcome the difference in the concentrations of those carriers. Indeed, albumin is the most abundant plasma protein (~0.5-0.8 mM) whereas lipoprotein concentration is much lower (~1 µM for LDL and 13µM for HDL).

Despite presumed protein-affinity of hydrophilic compounds, there is no correlation between affinity towards HSA and CHI. Hydrophilic compounds, such as TPP(*m*O□GluOH)$_4$, present low binding constants but it is also the case of most hydrophobic structures such as TPP(*m*OH)$_3$. Highest binding constants are characteristic of compounds (TPP(*p*OH)$_4$, TPP(*m*OH)$_4$ or TPP(*p*O□GalOH)$_3$) with intermediate hydrophobicities. On the contrary, TPPs' affinity towards lipoproteins can be globally accounted for by their hydrophobicity. Affinity increase with CHI applies both to HDL and LDL but is more pronounced in the case of the latter. This observation can be linked to the classical idea of a preferential binding of more hydrophobic structures to LDL. However, this rule knows exceptions and in the studied series, despite correlation of affinity with CHI, proportion of LDL-binding is not correlated with hydrophobicity. The latter fact is the consequence of the absence of correlation between affinity towards HSA and CHI.

Similar considerations should explain an exception to the classical rule reported by Hasan. Protoporphyrin and hematoporphyrin bind in the same proportions to plasma proteins despite the higher hydrophobicity of the former. This result must be viewed as the consequence of the difference in substitution which confers a much higher affinity towards albumin for protoporphyrin (280.10^6 M^{-1}) than for hematoporphyrin ($1,4.10^6$ M^{-1}). This albumin affinity increase counterbalances the probable hydrophobicity-induced increase in affinity towards lipoproteins, resulting in a similar plasma distribution.

426

427 **4.3. Interactions with Human Serum Albumin**

428 Contrary to HDL- and LDL-affinities, an increase in hydrophobicity doesn't result in an
429 increased affinity towards albumin. Confronted with similar observations, some authors have
430 underlined the importance of the amphiphilic character of the photosensitizer in its
431 interactions with proteins [30]. Those conclusions strengthen the interest of docking
432 simulations to better understand phenomena governing interactions between TPPs and HSA.
433 Docking results have shown that substitution affects location of the TPP derivative on the
434 protein. Moreover, they have led to exclude interactions at classical drug binding sites I and
435 II, unlike what has been described for some sensitizers: chlorin p6, purpurin 18 [32] or
436 bacteriochlorin derivatives [33]. This difference probably results from steric difference
437 between those tetrapyrroles not bearing phenyles at meso positions and the bulky TPP core.
438 Results obtained with other tetra-*para*substituted TPPs conclude to a binding at the surface
439 of the albumin molecule, a result consistent with our findings. Fluorescence lifetime studies
440 performed on a series of sulfonated phthalocyanines have shown that degree of sulfonation
441 influences insertion in hydrophobic pockets. Tetrasulfonated derivative bind at the surface of
442 the protein whereas lower sulfonation degree allows insertion into hydrophobic cavities [34].
443 However, effect of substituent is only partly steric. It also plays a role in interactions
444 modalities between sensitizer and HSA. Sulfone groups could form ionic interactions with
445 basic amino acids (histidine and lysine), an hypothesis strengthened by sensitivity of
446 interactions to ionic strength [35].
447 The double acting effect of the substituent, likely to form direct interactions with HSA but also
448 to induce steric limitations, also applies to our series of hydroxylated and glycoconjugated
449 porphyrins. Glycoconjugated derivatives form more hydrogen bonds than hydroxylated ones,
450 and *meta*-derivatives more than *para*-derivatives. However, even when glycoconjugated,
451 TPP derivatives interact with the protein mainly through hydrophobic interactions. The direct
452 involvement of the substituent in the binding distinguishes TPP interactions with proteins
453 from their interactions with the C18 surface in the HPLC experiments. Indeed, CHI values are

454 highly correlated with ratios of TPP nucleus surface to the total TPP derivatives surface (r^2 =
455 0,94 when excluding the highly flexible TPP(*p*ODEGO□ManOH)$_3$), which illustrates the
456 probable lack of direct interactions between the substituent and apolar surfaces. In the case
457 of interactions with albumin, susbtituents interact directly with the protein, especially if the
458 TPP derivative possesses some flexibility (case of *meta*-derivatives and
459 TPP(*p*ODEGO□ManOH)$_3$). Rigidity of planar *para*-derivatives prevents them to form specific
460 interactions with albumin, which could explain the absence of difference in distribution
461 pattern between TPP(*p*O□GalOH)$_4$ and TPP(*p*O□GluOH)$_4$ despite modification of the nature
462 of sugar residue. This observation also applies to the respective affinities of those particular
463 derivatives.
464 When compared with the more widespread distribution pattern of *para*-derivatives, *meta*-
465 derivatives seem to present stronger and more specific interactions. This result, conflicting at
466 the first sight with affinity constants (higher in the *para* series), should maybe be considered
467 differently: globular conformation of *meta*-derivatives prevents them from interacting at the
468 surface of albumin molecule, thus restraining their possible binding sites. In this perspective,
469 higher overall binding constants measured on *para*-derivatives could result from a higher
470 number of sites of almost equivalent affinities.
471

472 **4.4. Considerations about the particular affinity for LDL**

473 Photosensitizers are likely to interact with lipoproteins according to two modes, whether with
474 the proteic portion and/or with the lipidic one [36]. Existence of high affinity sites on
475 apoprotein coexisting with secondary solubilization in lipidic portion has been supposed in
476 the case of interactions of chlorin e6 with LDL [37]. If global binding constant is of the same
477 order of magnitude than that obtained for glycoconjugated TPPs, a preferential binding to
478 apoprotein is unlikely for the latters. Good correlation between affinity towards lipoproteins
479 and hydrophobicity tend to privilegiate the idea of an interaction with the lipidic portion. It
480 seems probable that interactions of TPPs with the hydrophobic stationnary phase in HPLC
481 are quite similar to their interactions with the hydrophobic lipidic portion. Moreover, lower

binding affinity towards lipoproteins of glycoconjugated derivatives – likely to interact strongly with proteic portion through hydrogen bonding – reinforces the hypothesis of an interaction with the lipidic portion. At last, this hypothesis is confirmed by comparison with affinities of TPPs towards liposomes [38]. Ranking of binding affinities towards those phospholipidic vesicules is close to that obtained with HDL.

Difference in binding affinities towards HDL and LDL leads to consider a possible role of certain lipids in the preferential binding of TPPs to LDL than HDL. Interactions of hypericin with biological membranes have shown that this structure presents a particular affinity for cholesterol [39], a fact that could account for its location in LDL, between hydrophobic core and phospholipid shell [40]. Involving cholesterol is unlikely for our compounds, more amphiphilic than hypericin, and thus less able to insert deeply in the lipoprotein core. This hypothesis is supported by studies of inclusion of dendrimeric porphyrins in biological membranes, that show no impact of cholesterol proportion [41], contrary to what could have been described for others photosensitizers, such as deuteroporphyrin [42]. Preferential affinity for LDL than for HDL could result from differences in surface properties: LDL surface is less hydrophobic and its outer layer is more fluid [43]. More hydrophobic character of HDL surface results from the presence of more triglycerides and cholesterol esters in the outer layer [44]. Combined together, amphiphilic structures could better interact with LDL, insertion of hydrophobic pole being easier and interaction of hydrophilic part with the surface being favored.

5. Conclusion

Those observations give a new insight in plasma distribution. Increasing hydrophobicity should orientate distribution towards LDL, whereas lowering this parameter results in a majoritary protein binding. Exceptions to this rule should result from specific interactions between a photosensitizer and a carrier, interactions not directly related to its hydrophobicity. Our study also shows that measuring the fraction bound to LDL is not sufficient to understand the behavior of TPPs in plasma. Binding constant determinations are essential. If

it is commonly admitted that plasma distribution plays a decisive role in orientating biodistribution, binding affinities are likely to affect photosensitizer's ability to pass from the carrier to its final target, a fact that should not be underestimateed when reconsidering the link between plasma behavior and tumor localization.

6. Acknowledgements

B. Chauvin has benefited from a "Postes d'accueil CNRS – CEA – APHP" grant. The authors thank technicians of HEGP Biochemistry service for their precious contribution to plasma distribution studies.

7. References

[1] T.J. Dougherty, C.J. Gomer, B.W. Henderson, G. Jori, D. Kessel, M. Korbelik, J. Moan, Q. Peng, J. Natl. Cancer Inst, 90 (1998) 889-905.

[2] F. Doz, H. Brisse, D. Stoppa-Lyonnet, X. Sastre, J. Zucker, L. Desjardins, *Retinoblastoma in: Paediatric Oncology*, Pinkerton, R Plowman, N Pieters, R, London, 2004.

[3] J.B. Winther, Acta Ophthalmol Suppl, (1990) 1-37.

[4] M.-C. Desroches, A. Bautista-Sanchez, C. Lamotte, B. Labeque, D. Auchère, R. Farinotti, P. Maillard, D.S. Grierson, P. Prognon, A. Kasselouri, J. Photochem. Photobiol. B, Biol, 85 (2006) 56-64.

[5] P. Maillard, B. Loock, D. Grierson, I. Laville, J. Blais, F. Doz, L. Desjardins, D. Carrez, J. Guerquinkern, A. Croisy, Photodiagnosis and Photodynamic Therapy, 4 (2007) 261-268.

[6] M. Lupu, C.D. Thomas, P. Maillard, B. Loock, B. Chauvin, I. Aerts, A. Croisy, E. Belloir, A. Volk, J. Mispelter, Photodiagnosis and Photodynamic Therapy, 6 (2009) 214-220.

[7] B. Chen, B.W. Pogue, P.J. Hoopes, T. Hasan, Int. J. Radiat. Oncol. Biol. Phys, 61 (2005) 1216-1226.

[8] M.R. Horsman, J. Winther, Acta Oncol, 28 (1989) 693-697.

[9] F. Danhier, O. Feron, V. Préat, Journal of Controlled Release, 148 (2010) 135-146.

[10] W.G. Roberts, T. Hasan, Cancer Res, 52 (1992) 924-930.

[11] G. Jori, L. Schindl, A. Schindl, L. Polo, Journal of Photochemistry and Photobiology A: Chemistry, 102 (1996) 101-107.

[12] J.T.C. Wojtyk, R. Goyan, E. Gudgin-Dickson, R. Pottier, Medical Laser Application, 21 (2006) 225-238.

[13] T. Hasan, B. Ortel, A.C. Moor, B.W. Pogue, dans: Cancer medicine 6, BC Decker, Hamilton Ont. ;;Lewiston NY, 2003.

[14] B.A. Allison, P.H. Pritchard, A.M. Richter, J.G. Levy, Photochem. Photobiol, 52 (1990) 501-507.

[15] H.J. Hopkinson, D.I. Vernon, S.B. Brown, Photochem. Photobiol, 69 (1999) 482-488.

[16] A.P. Castano, T.N. Demidova, M.R. Hamblin, Photodiagnosis and Photodynamic Therapy, 2 (2005) 91-106.

[17] I. Laville, T. Figueiredo, B. Loock, S. Pigaglio, P. Maillard, D.S. Grierson, D. Carrez, A. Croisy, J. Blais, Bioorg. Med. Chem, 11 (2003) 1643-1652.

[18] I. Laville, S. Pigaglio, J.-C. Blais, B. Loock, P. Maillard, D.S. Grierson, J. Blais, Bioorg. Med. Chem, 12 (2004) 3673-3682.

[19] I. Laville, S. Pigaglio, J.-C. Blais, F. Doz, B. Loock, P. Maillard, D.S. Grierson, J. Blais, J. Med. Chem., 49 (2006) 2558-2567.

[20] D. Oulmi, P. Maillard, J.-L. Guerquin-Kern, C. Huel, M. Momenteau, J. Org. Chem., 60 (1995) 1554-1564.

[21] K. Valko, C. Bevan, D. Reynolds, Anal Chem, 69 (1997) 2022-2029.

[22] Q. Wang, H.J. Altermatt, H.B. Ris, B.E. Reynolds, J.C. Stewart, R. Bonnett, C.K. Lim, Biomed. Chromatogr, 7 (1993) 155-157.

[23] T. Ohnishi, N.A.L. Mohamed, A. Shibukawa, Y. Kuroda, T. Nakagawa, S. El Gizawy, H.F. Askal, M.E. El Kommos, J Pharm Biomed Anal, 27 (2002) 607-614.

[24] A. de Juan, R. Tauler, Critical Reviews in Analytical Chemistry, 36 (2006) 163 - 176.

[25] J. Diewok, A. de Juan, M. Maeder, R. Tauler, B. Lendl, Anal. Chem., 75 (2003) 641-647.

[26] *R Development Core Team, R: A Language and Environment for Statistical Computing*, R Foundation for Statistical Computing, Vienna, Austria, 2009.

[27] I.H. van Stokkum, K.M. Mullen, V.V. Mihaleva, Chemometr. Intell. Lab., 95 (2009) 150-163.

[28] O. Trott, A.J. Olson, J Comput Chem, 31 (2010) 455-461.

[29] M. Kongshaug, J. Moan, Int J Biochem Cell Biol, 21 (1995) 371-384.

[30] O. Rinco, J. Brenton, A. Douglas, A. Maxwell, M. Henderson, K. Indrelie, J. Wessels, J. Widin, Journal of Photochemistry and Photobiology A: Chemistry, 208 (2009) 91-96.

[31] W. An, Y. Jiao, C. Dong, C. Yang, Y. Inoue, S. Shuang, Dyes and Pigments, 81 (2009) 1-9.

[32] S. Patel, A. Datta, J Phys Chem B, 111 (2007) 10557-10562.

[33] Y. Chen, R. Miclea, T. Srikrishnan, S. Balasubramanian, T.J. Dougherty, R.K. Pandey, Bioorg. Med. Chem. Lett, 15 (2005) 3189-3192.

[34] K. Lang, J. Mosinger, D.M. Wagnerova, Coordination Chemistry Reviews, 248 (2004) 321-350.

[35] A. Filyasova, I. Kudelina, A. Feofanov, Journal of Molecular Structure, 565-566 (2001) 173-176.

[36] S. Bonneau, C. Vever-Bizet, P. Morlière, J.-C. Mazière, D. Brault, Biophysical Journal, 83 (2002) 3470–3481.

[37] H. Mojzisova, S. Bonneau, C. Vever-Bizet, D. Brault, Biochim. Biophys. Acta, 1768 (2007) 366-374.

[38] H. Ibrahim, A. Kasselouri, C. You, P. Maillard, V. Rosilio, R. Pansu, P. Prognon, Journal of Photochemistry and Photobiology A: Chemistry, 217 (2011) 10-21.

[39] Y.-F. Ho, M.-H. Wu, B.-H. Cheng, Y.-W. Chen, M.-C. Shih, Biochimica et Biophysica Acta (BBA) - Biomembranes, 1788 (2009) 1287-1295.

[40] G. Lajos, D. Jancura, P. Miskovsky, J. Garcia-Ramos, S. Sanchez-Cortes, Journal of Physical Chemistry C, 113 (2009) 7147-7154.

[41] A. Makky, J.P. Michel, S. Ballut, A. Kasselouri, P. Maillard, V. Rosilio, Langmuir, 26 (2010) 11145-11156.

[42] K. Kuzelova, D. Brault, Biochemistry, 34 (1995) 11245-11255.

[43] J.B. Massey, H.J. Pownall, Biophys. J, 74 (1998) 869-878.

[44] L.S. Kumpula, J.M. Kumpula, M.-R. Taskinen, M. Jauhiainen, K. Kaski, M. Ala-Korpela, Chem. Phys. Lipids, 155 (2008) 57-62.

Figure 1. Structure of *meso*-tetraphenylporphyrin derivatives

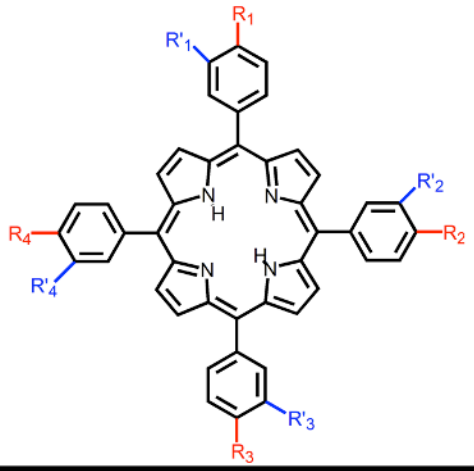

meta-substituted compounds				
$R_1 = R_2 = R_3 = R_4 = -H$	R'_1	R'_2	R'_3	R'_4
TPP(*m*OH)$_3$	-OH	-OH	-OH	-H
TPP(*m*OH)$_4$	-OH	-OH	-OH	-OH
TPP(*m*OβGluOH)$_3$	-OβGluOH	-OβGluOH	-OβGluOH	-H
TPP(*m*OβGluOH)$_4$	-OβGluOH	-OβGluOH	-OβGluOH	-OβGluOH
para-substituted compounds				
$R'_1 = R'_2 = R'_3 = R'_4 = -H$	R_1	R_2	R_3	R_4
TPP(*p*OH)$_3$	-OH	-OH	-OH	-H
TPP(*p*OH)$_4$	-OH	-OH	-OH	-OH
TPP(*p*OβGalOH)$_3$	-OβGalOH	-OβGalOH	-OβGalOH	-H
TPP(*p*OβGalOH)$_4$	-OβGalOH	-OβGalOH	-OβGalOH	-OβGalOH
TPP(*p*OβGluOH)$_4$	-OβGluOH	-OβGluOH	-OβGluOH	-OβGluOH
TPP(*p*ODEGOαManOH)$_3$	-ODEGOαManOH	-ODEGOαManOH	-ODEGOαManOH	-H

Figure 2. Spectral modifications of TPP(*p*O□GalOH)$_3$ upon binding to HSA

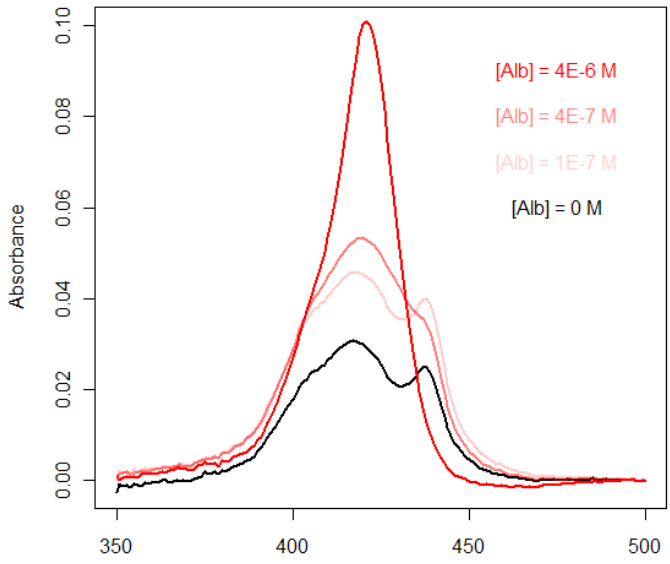

603 **Figure 3**. Conformations of *meta*- and *para*- derivatives

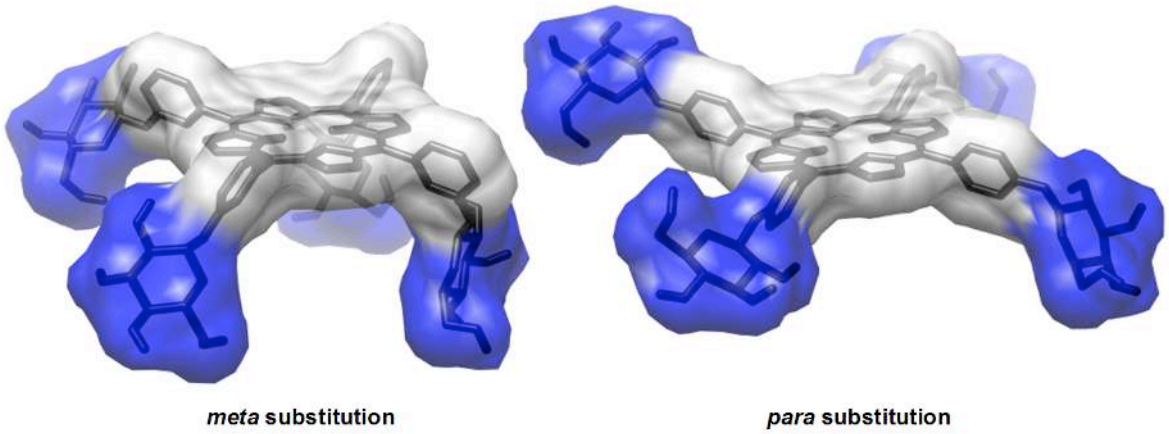

604

605

606

Figure 4. Binding sites of glycoconjugated TPPs according to blind docking results

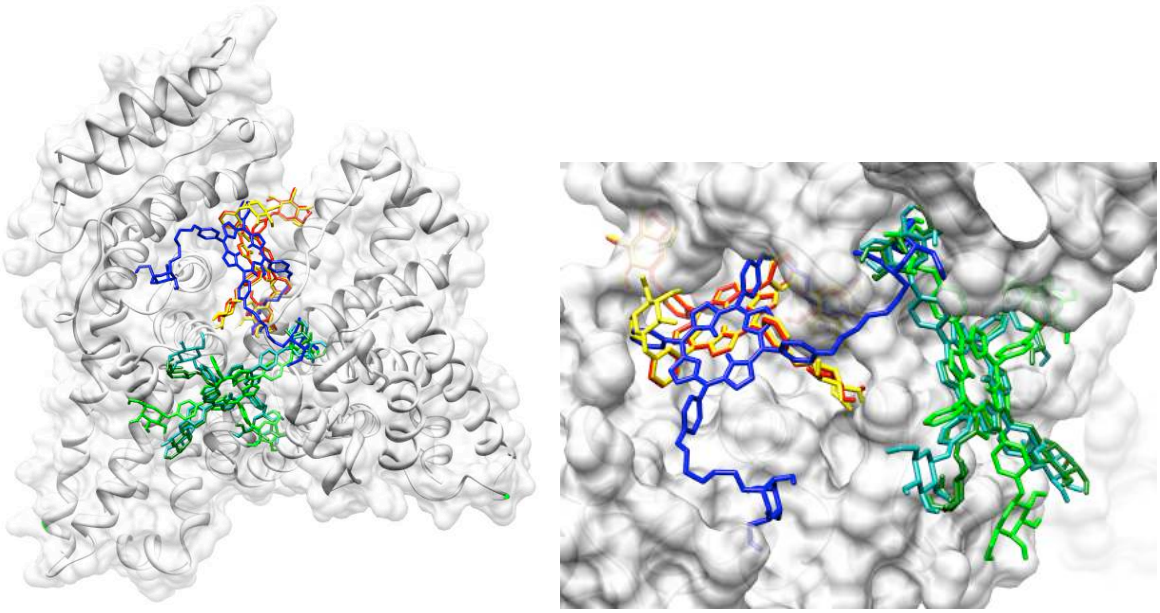

Binding sites of TPP(*m*O□GluOH)$_3$ (in red), TPP(*m*O□GluOH)$_4$ (in yellow), TPP(*p*O□GalOH)$_3$ (in green), TPP(*p*O□GalOH)$_4$ (in dark green), TPP(*p*O□GluOH)$_4$ (in sea green) and TPP(*p*ODEGO□ManOH)$_3$ (in blue)

Table 1. Plasma distribution of *meso*-tetraphenylporphyrin derivatives

Compound		Lipoproteins			Proteins
	CHI	Total	HDL	LDL	
TPP(*m*OH)$_3$	-	94.7 ± 1.3	74.2 ± 5.2	17.3 ± 4.8	5.3 ± 1.3
TPP(*m*OH)$_4$	117.2 ± 0.1	97.6 ± 0.4	71.3 ± 1.0	20.0 ± 3.0	2.4 ± 0.4
TPP(*m*O□GluOH)$_3$	55.7 ± 0.5	97.8 ± 1.0	78.0 ± 4.9	14.1 ± 3.4	2.2 ± 1.0
TPP(*m*O□GluOH)$_4$	39.3 ± 0.1	95.6 ± 1.2	60.8 ± 13.0	22.1 ± 5.4	4.4 ± 1.2
TPP(*p*OH)$_3$	-	95.0 ± 1.2	77.6 ± 4.7	13.4 ± 3.0	5.0 ± 1.2
TPP(*p*OH)$_4$	100.2 ± 0.2	96.4 ± 1.3	86.7 ± 5.4	7.7 ± 4.0	3.6 ± 1.3
TPP(*p*O□GalOH)$_3$	40.8 ± 0.1	77.3 ± 1.6	67.7 ± 2.1	7.1 ± 1.1	22.7 ± 1.6
TPP(*p*O□GalOH)$_4$	26.5 ± 0.1	10.4 ± 1.4	8.7 ± 1.6	1.4 ± 0.5	89.6 ± 1.4
TPP(*p*O□GluOH)$_4$	28.3 ± 0.1	13.7 ± 4.2	11.3 ± 3.6	1.8 ± 0.4	86.3 ± 4.2
TPP(*p*ODEGO□ManOH)$_3$	62.4 ± 0.1	95.4 ± 1.3	85.8 ± 3.0	8.6 ± 4.0	4.6 ± 1.3

613 **Table 2**. Binding affinities of *meso*-tetraphenylporphyrin derivatives (expressed as log K_a)

Compound	CHI	Albumin		Lipoproteins	
		HSA	HSAlip	LDL	HDL
TPP(*m*OH)$_3$	-	5.07	5.50	8.30	8.11
TPP(*p*OH)$_3$	-	5.60	5.77	8.32	7.11
TPP(*m*OH)$_4$	117.2 ± 0.1	5.77	5.99	8.21	7.65
TPP(*p*OH)$_4$	100.2 ± 0.2	6.32	6.17	8.77	7.35
TPP(*p*ODEGO□ManOH)$_3$	62.4 ± 0.1	4.90	5.19	7.78	7.01
TPP(*m*O□GluOH)$_3$	55.7 ± 0.5	5.66	5.73	7.64	7.33
TPP(*p*O□GalOH)$_3$	40.8 ± 0.1	5.80	6.17	7.89	7.33
TPP(*m*O□GluOH)$_4$	39.3 ± 0.1	5.05	5.03	7.58	6.95
TPP(*p*O□GluOH)$_4$	28.3 ± 0.1	5.57	5.83	6.87	6.51
TPP(*p*O□GalOH)$_4$	26.5 ± 0.1	5.29	5.27	6.80	6.33

614

615

615

616 **Table 3**. Properties of interface surfaces between HSA and the different TPP derivatives

	Interface surface			Percentage of the TPP surface involved in the interaction	Contribution of the substituent in the interaction[1]
	Polar	Apolar	Total		
TPP	129.6	315.1	444.7	35.1%	0.0%
TPP(*m*O□GluOH)$_3$	296.3	412.4	708.7	34.4%	64.4%
TPP(*m*O□GluOH)$_4$	391.1	530.3	921.4	32.9%	62.6%
TPP(*m*OH)$_3$	121.9	297.1	419.0	37.7%	11.5%
TPP(*m*OH)$_4$	134.7	271.4	406.1	42.9%	23.4%
TPP(*p*O□GalOH)$_3$	200.6	404.7	605.3	27.9%	55.5%
TPP(*p*O□GalOH)$_4$	276.2	305.2	581.4	25.9%	52.7%
TPP(*p*O□GluOH)$_4$	260.3	304.7	564.9	29.0%	54.3%
TPP(*p*OH)$_3$	97.4	234.2	331.5	28.0%	11.4%
TPP(*p*OH)$_4$	94.7	216.4	311.1	24.5%	11.5%
TPP(*p*ODEGO□ManOH)$_3$	352.9	464.5	817.4	30.6%	69.5%

617 1. Defined as the ratio between the surface of the substituent in contact with the protein and
618 the total surface of the TPP derivative interacting with the protein

619